Altered gray-white matter boundary in toddlers at risk for autism relates to later diagnosis of Autism Spectrum Disorder.

Michel Godel (michel.godel@unige.ch)
Universite de Geneve Faculte de Medecine https://orcid.org/0000-0002-9789-3540
Derek Sayre Andrews
MIND Institute: University of California Davis MIND Institute
David Gil Amaral
MIND Institute: University of California Davis MIND Institute
Sally Ozonoff
MIND Institute: University of California Davis MIND Institute
Gregory S. Young
MIND Institute: University of California Davis MIND Institute
Joshua K. Lee
MIND Institute: University of California Davis MIND Institute
Christine Wu Nordahl
MIND Institute: University of California Davis MIND Institute
Marie Schaer
University of Geneva Medical Centre: Universite de Geneve Faculte de Medecine

Research

Keywords: Autism Spectrum Disorder, Sibling risk, Toddlers, Neurodevelopment, Neuroimaging, FreeSurfer

Posted Date: December 2nd, 2020

DOI: https://doi.org/10.21203/rs.3.rs-118792/v1

Abstract

Background: Recent neuroimaging studies have highlighted differences in cerebral maturation in individuals with autism spectrum disorder (ASD) in comparison to typical development. For instance, the sharpness of the gray-white matter boundary is decreased in adults with ASD. To determine how the gray-white matter boundary integrity relates to early ASD phenotypes, we used a regional structural MRI index called the gray-white matter contrast (GWC) on a sample of toddlers with a hereditary high risk for ASD.

Methods: We used a surface-based approach to compute vertex-wise GWC in a longitudinal cohort of toddlers at high-risk for ASD imaged twice between 12 and 24 months (n=20). A full clinical assessment of ASD-related symptoms was performed in conjunction with imaging and again at three years of age for diagnostic outcome. Three outcome groups were defined (ASD, n=9; typical development, n=8; non-typical development, n=3).

Results: ASD diagnostic outcome at age 3 was associated with widespread increases in GWC between age 12 and 24 months. Many cortical regions were affected, including regions implicated in social processing and language acquisition. In parallel, we found that early onset of ASD symptoms (i.e. prior to 18-months) was specifically associated with slower GWC rates of change during the second year of life. These alterations were found in areas mainly belonging to the central executive network.

Limitations: Our study is the first to measure maturational changes in GWC in toddlers who developed autism, but the limited size of our sample warrants further replication in independent and larger samples.

Conclusion: These results suggest that ASD is linked to early alterations of the gray-white matter boundary in widespread areas. Early onset of symptoms constitutes an independent clinical parameter associated with a specific corresponding neurobiological developmental trajectory. Altered neural migration and/or altered myelination processes potentially explain these findings.

Background

Autism Spectrum Disorder (ASD) is a heterogeneous neurodevelopmental disorder characterized by difficulties in the domains of social interactions and communication, along with repetitive behaviors and restricted interests (1)(2). ASD affects 1 in 59 individuals with an increasing prevalence over the past decades (3)(4). Etiological mechanisms of ASD are thought to be mainly due to complex interactions of genetic predisposition and environmental risk factors, but have not been fully elucidated (5). It is now established that early intensive specific intervention can result in lasting positive outcomes (6). Despite recent improvement in symptom screening tools and procedures, often the age of ASD diagnoses still remains too late to capitalize on a critical therapeutic window for intervention (7)(8). Even when specific intervention is delivered early, clinical response is highly variable between toddlers for reasons that are not fully explained ye (9). Urgency for earlier diagnosis, intervention and more targeted therapeutic recommendations have led researchers to explore early behavioral and neurobiological markers of ASD.

Siblings of individuals with ASD share common genetic variants and exhibit an estimated risk of 18% to develop the disorder (10). Studies on these children at high risk for ASD (HR) have allowed a better characterization of early clinical signs and trajectories of ASD (11). For example, we now know that the first reliable signs of ASD usually emerge during the second year of life (12) and are often preceded by less specific atypical behaviors in

infancy (13). While diagnoses made at 18 months are stable and reliable, there is considerable variation in timing of symptom presentation. For example, approximately two-thirds of children who ultimately receive an ASD diagnosis will not demonstrate the full clinical picture yet at this age (14). This reduced clinical sensitivity of the early ASD behavioral phenotype has motivated the exploration of neuroimaging endophenotypes that could precede the emergence of symptoms and thus support clinical investigations (15) as well as earlier identification of risk. Several magnetic resonance imaging (MRI) studies have found that children aged from 6 to 24 months with ASD exhibited a larger volume of extra-axial cerebrospinal fluid compared to typically developing children (TD) (16) (17). F Faster cortical surface expansion in infancy followed by brain volume overgrowth during the second year of life has also been shown to be predictive of later ASD diagnosis (18). Moreover, higher fractional anisotropy values at the age of 6 months and decreased values after 12 months in various deep white matter tracts such as the corpus callosum and inferior longitudinal fasciculus have also been associated with later diagnosis of ASD (19) (20). Despite these promising results, the imaging literature exploring early brain developmental signatures of later ASD diagnosis is still sparse. Furthermore, all the mentioned studies have focused on global morphological metrics, such as extra-axial cerebrospinal fluid volume or mean fractional anisotropy of major fiber tracts. To our knowledge, no studies have explored regional developmental differences in this population through either vertex-wise or voxel-wise methods to date.

In adults with ASD, alterations of the boundary between cerebral gray and white matter in widespread cortical areas have been identified using various methodological approaches. In histological studies less clear delineation of the transition between gray and white structures has been described in postmortem tissue of adult patients with ASD (21). *In vivo* assessment of the gray-white matter boundary has been conducted using an MRI morphometric based measure called the gray-white matter intensity contrast (GWC) (22). GWC was first introduced in neurodegenerative imaging studies and has been extensively explored in aging populations (23). In neurodevelopmental studies, GWC has been found decreased in many regions in school-aged children and adults with ASD, (24) whereas adolescents with ASD exhibited similar GWC values compared to their peers with TD (24) (25). A more recent study reported increased GWC in adults with ASD, mostly in primary cortices (26). Although still sparse and somewhat inconsistent, existing literature suggests that GWC is likely decreased in many secondary cortices amongst children and adults with ASD and increased in some primary cortical regions.

Currently, the precise biological mechanisms underlying these alterations is unknown. GWC alterations in autism have largely been attributed to neural migration deficits. This interpretation is further supported by the rich literature about abnormal migration of neurons in ASD (27). Identification of alterations in GWC very early in life would support this hypothesis, but to date, there have been no studies evaluating GWC in very young infants or toddlers with later ASD outcomes. One study in young TD toddlers reported increased GWC rates of change in areas relevant for language development between 12 and 19 months (e.g. the left superior temporal sulcus) (28). To our knowledge, apart from this report, GWC trajectories during the first years of life have never been assessed either in TD or ASD.

In the current study, we explored how GWC is associated with various ASD-related clinical parameters in a longitudinal cohort of HR infants to explore the potential of GWC as an early biomarker of diagnostic outcome and symptom severity. Each participant underwent two MRI scans between the age of 12 and 24 months. We performed a quantitative whole-brain surface-based exploratory analysis. Given the lack of previous studies using GWC in children with ASD younger than 2, we didn't have any *a priori* hypotheses regarding the location and direction of potential alterations. We assessed whether GWC was correlated with symptom severity at the

time of the scan acquisition, and whether this was predictive of clinical diagnostic outcome at 36 months of age. Given the heterogeneity of age at which reliable behavioral symptoms of ASD first emerge (14), we performed further analyses to evaluate associations between the age of symptom onset and GWC alterations. We hypothesized that if GWC alterations were to be found, they would be more prominent amongst ASD children experiencing an early onset (i.e., prior to 18 months of age) of ASD symptoms (EOA) compared to children with later onset of ASD symptoms (LOA).

Material And Methods

We used an MRI dataset from participants recruited through the UC Davis MIND Institute between 2009 and 2011. The recruitment process as well as clinical and imaging procedures have been described in detail previously (16).

Participants

Between 2009 and 2011, participants from a clinical longitudinal cohort (29) were asked to also take part in an MRI acquisition protocol. Invitation was made through phone screening and led to the recruitment of 64 participants. For these longitudinal analyses, we first selected the 41 participants who were categorized as HR (13 females). In this study, HR was defined as having an older sibling with a confirmed diagnosis of ASD. Having a sample exclusively constituted of HR participants allows to study the continuum of symptom severity and the emergence of ASD amongst participants who share a similar risk to develop the disorder (10). For our analysis, we included only the 22 HR participants who underwent 2 MRI scans (first at 12–15 months and second at 18–24 months of age). From this longitudinal sample, 2 children had to be excluded due to poor image quality, resulting in a final sample of 20 HR children (5 females).

Demographic characteristics of the sample are displayed in Table 1. We divided our sample into three groups according to their diagnostic outcome at age 3: HR with typical development (HR-TD, n = 8, 3 females), HR with ASD (HR-ASD, n = 9, 1 female) and HR with atypical development (HR-non-TD, n = 3, 1 female). One HR-TD child did not undergo the 18-month clinical assessment but was not excluded from the study. We further separated HR-ASD participants into two subgroups according to age of first established diagnosis. HR-ASD who were diagnosed at 18 months or before were classified as early onset autism (EOA; n = 4, 1 female). HR-ASD participants whose diagnosis was established later than 18 months of age were labelled as later onset autism (LOA; n = 5, 0 female).

Behavioral Measures And Outcome Classification

Clinical assessments were conducted with each participant at 6, 12, 18, 24 and 36 months. Only assessments at 18 and 36 months of age were considered in the current study.

The Mullen Scales of Early Learning (MSEL) was used to assess development in cognitive (expressive and receptive language, visual reasoning) and motor (fine and gross) areas (30). Developmental quotient scores (DQ) were used instead of standard scores in order to limit truncation of very low performing participants (31). Individual DQs were obtained by dividing age-equivalent developmental age output from MSEL by chronological age and multiplying by 100.

ASD-related symptom severity was quantified with the Autism Diagnostic Observation Schedule (ADOS) (32). The ADOS is a semi-structured observational evaluation with cut-offs to guide diagnostic decisions, appropriate for ambulatory children of 12 months and older. Either module 1 (intended for non-verbal children or those using only isolated words) or module 2 (intended for children with phrase speech) was conducted at ages 18, 24 and 36 months. To allow comparison of ADOS total scores across ages and modules, the calibrated severity score (CSS) was used. ADOS CSS ranges from 1 to 10 (with 10 being the most severe) (33)(34).

At each visit from 18 months and later, ASD diagnosis outcome was established by a licensed clinician according to ADOS diagnosis cut-offs and DSM-IV criteria (35). Children who did not meet the criteria for a diagnosis of ASD were categorized as having typical development (TD) or non-typical development (non-TD). TD was defined as having an ADOS CSS equal to or less than 2, a total DQ of at least 85, no DQ subtest less than 80 and no more than one DQ subtest less than 85. If one or more of these criteria were not met, participants without ASD were classified as non-TD.

Image Acquisitions

All children were scanned during natural sleep following previously published procedures (36), at the UC Davis Imaging Research Centre on a 3 T Siemens TIM Trio MRI system with an eight-channel head coil. Structural T1-weighted 3D MP-RAGE images were acquired with 1 mm^3 isometric voxels, repetition time = 3200 ms, echo time = 5.08 ms, field of view = 176 mm and 192 sagittal slices. The success rate of these MRI acquisitions was 78%. A 3D image distortion map (Image Owl) was acquired at the end of each scan with a calibration phantom (Phantom Laboratory, Inc.). Distortion correction was carried out as described in (37).

Participants had a first MRI scan at 6–9 months of age which was not evaluated in the present analyses because of the difficulty to obtain accurate 3D white matter surface reconstructions at this age. Accordingly, we utilized the participant's second scan, acquired between 12 and 15 months of age, and third scan, acquired between 18 and 24 months of age.

Image Processing

We used the automated pipeline provided by FreeSurfer v6.0 to process the T1-weighted cerebral MRIs (http://surfer.nmr.mgh.harvard.edu/). The successive steps of this automated procedure are described in detail elsewhere (38)(39)(40)(41). Briefly, non-cerebral tissues are removed, signal intensity is normalized, and the image is segmented using a connected components algorithm. Then, a single filled volume of white matter is generated for each hemisphere. For each volume of white matter, a triangular surface tessellation is created by fitting a deformable template. Through deformation of this tessellated surface, a cortical mesh is created that defines the boundary between white and cortical gray matter (called the outer white matter surface) as well as the boundary between the gray matter and the extra-axial fluid (called the pial surface). This surface deformation process is calculated through an energy minimization function that determines the sharpest shift in intensity between voxels to define the transition between tissue categories. This process is independent of absolute intensity values and can delineate boundaries at a subvoxel resolution.

A trained operator (M.G.), blind to any clinical outcome, visually inspected images obtained with the described automated pipeline. When required, manual corrections were implemented following recommended procedures

described in the FreeSurfer manual (http://freesurfer.net/fswiki/). All final cortical surfaces were visually validated by a second trained independent operator (M.S.) who was also blind to all clinical outcomes.

Gray-white Matter Intensity Contrast

We first sampled white matter intensity at each vertex *v* at 1mm beneath the white matter (WM) outer surface (Fig.1). A distance of 1mm was chosen to facilitate comparisons with previous literature since it is the most commonly used value in GWC studies, including all existing studies exploring GWC in ASD (25) (26). Gray matter (GM) intensity value was sampled at each vertex at a distance of 30% of cortex width (defined as the distance between outer white matter surface and pial surface) starting from the white matter outer surface. The value of 30% was set because it is the most commonly used in the GWC literature (25) and is the default value provided by FreeSurfer. In addition, a previous study of ASD found diagnostic differences to be greatest when GM intensity sampled between 30 and 40% was used to compute GWC (26). GWC at each vertex *v* was computed by dividing the difference between GM and WM intensities by the mean between GM and WM intensities and multiplying by 100 to get a ratio expressed in [%].

$$\mathrm{GWC}_v\,[\%] = 100 \times \frac{(WM_v - GM_v)}{(WM_v + GM_v)/2} \qquad (1)$$

GWC values were then registered on an average template provided by FreeSurfer to allow vertex-wise inter-participants comparison. During this process, GWC values were smoothed with a full-width at half-maximum (FWHM) surface-based Gaussian kernel of 10 mm.

Then, for each participant two different GWC longitudinal values were computed. Longitudinal neuroimaging pipelines allow many advantages over cross-sectional designs, including reduction of within-participant variability and the possibility to analyze the effect of time on the variable of interest (42). The first longitudinal value was the mean GWC value at each vertex *v* between the two scans (mGWC). Mean GWC represents the vertex-wise mean GWC value between age 1 and 2.

$$\mathrm{mGWC}_v\,[\%] = \frac{GWC_v1 + GWC_v2}{2} \qquad (2)$$

Where GWC*v*1 is GWC*v* at 12-15 months and GWC*v*2 is GWC*v* at 18-24 month.

Second was GWC rate of change between two scans (ΔGWC). ΔGWC represents the effect of time on GWC between the age of 12 and 24 months. It was computed through the symmetrical percentage of change (SPC) formula (42). SPC consists of calculating for each participant at each vertex *v* the GWC difference between two scans divided by the age difference between the two scans, giving a rate in [%/month]. This rate is divided by mean GWC at each vertex *v* and multiplied by 100, giving a result expressed in [%]. One advantage of using SPC

value to express rate of change is that it is symmetrical (i.e. not more dependent on values of one of the two scans). SPC expresses the rate at which GWC changes in each vertex between two scans relative to mean GWC.

$$\Delta \mathrm{GWC}_v\,[\%] = 100 \times \frac{(GWC_v2 - GWC_v1)/(age2 - age1)}{mGWC_v} \quad (3)$$

Where *age1* is participant's age at 12-15 months scan and *age2* is their age at 18-24 months scan.

Cortical Thickness

Cortical thickness (CT) alterations have been found to influence GWC values (43). CT is defined by the distance in mm between WM outer surface and pial surface and is automatically computed by the standard FreeSurfer processing pipeline (41). To control for this possible confound, we sampled CT at each vertex v. We then computed the mean CT (mCT) and the CT rate of change (ΔCT) with the same formulas we described for longitudinal GWC parameters. Spatial overlap between significant effects on GWC and CT were explored.

Statistical analysis

Sample characteristics analyses

Our primary outcomes are symptom severity (ADOS CSS at 18 and 36 months of age) and discrete diagnosis at age 3 (HR-TD, HR-ASD, HR-non-TD). We further subdivided the HR-ASD into late and early symptom onset (LOA and EOA). Associations between clinical outcome and individual characteristics that could represent potential confounding factors in GWC analysis were explored. These parameters included gender, age at scanning (which was calculated as mean age between two scans) and time interval between scans. According to the nature of the tested variables (i.e. discrete or continuous), we used either Pearson correlation or one-way ANOVA or Student T-test (or Mann-Whitney U test when non-parametric distribution of variables was found) or chi-square test.

For descriptive purposes, we tested for differences in behavioral scores (DQ, ADOS CSS at 18 and 24 months) between diagnosis groups (HR-TD, HR-ASD and HR-non-TD) using one-way ANOVA. We also tested for potential differences in behavioral scores between the two HR-ASD subgroups (EOA and LOA) using either Student T-test or Mann-Whitney U test. Statistics described in this section were performed with Prism® v.8.3.0 software with significance threshold set at alpha = 0.05.

Surface-based Analyses

We used the general linear model (GLM) command implemented in FreeSurfer to perform vertex-wise whole-brain surface-based analysis of GWC.

First, to determine the effect of time on GWC in typical development between the age of 1 and 2, we performed vertex-wise parametric comparison of ΔGWC values *versus* zero in our HR-TD group. We then extracted vertex-wise ΔGWC values from all significant clusters and computed an average ΔGWC value for each hemisphere. This mean hemispheric ΔGWC value was compared between right and left to test for any asymmetry in the effect of age on GWC.

Then, we fit a GLM to test whether mean GWC or at age 12-24 months are associated with discrete diagnostic outcome at age 3 (HR-ASD-or HR-TD):

$$\mathrm{mGWC} \sim Diagnostic\ outcome\ +\ age\ ;\ \Delta\mathrm{GWC} \sim Diagnostic\ outcome\ +\ age \quad (4)$$

We further tested if symptom severity at 18 months of age (i.e. during the scan acquisition period going from 12 to 24 months of age) and at age 3 (36 months) were associated with GWC values. The following GLM was conducted:

$$\mathrm{mGWC} \sim ADOS\ CSS\ +\ age\ ;\ \Delta\mathrm{GWC} \sim ADOS\ CSS\ +\ age \quad (5)$$

Given that GWC before the age of 2 is influenced by age (28), age at scanning (calculated for each participant as the mean age between two scans) was regressed out in all GLM analyses. The p-value for each voxel was calculated using two-tailed testing with significance threshold set at alpha = 0.05. Cluster-wise analyses were corrected for multiple comparisons using Monte-Carlo simulation (MCS) with a significance threshold for cluster-wise p-value (CWP) of alpha = 0.05. We used cluster-wise and MCS analysis pipelines implemented in FreeSurfer (44).

We then wanted to determine if potential alterations of GWC (mean GWC and) found with GLM analysis were associated with the age at which the first ASD-related symptoms emerged. As a post-hoc analysis, for each cluster exhibiting significant GWC alterations (in either mean GWC or), we computed the average of all vertex-wise GWC values (respectively mean GWC or ΔGWC) across all vertices in the cluster for each participant. These individual cluster-averaged GWC values were then compared between HR-TD participants and each of the HR-ASD subgroups (EOA and LOA) using Student T-test or Mann-Whitney U. Significance threshold was set at alpha = 0.05.

The same GLM methods described here were also utilized for analyses of mCT and ΔCT values.

Results

Sample characteristics

Clinical characteristics of the sample are described in Table 1. As expected, the HR-ASD group exhibits the most severe symptom severity and the lowest DQ at age 3. There is no significant difference between groups in either DQ or symptom severity at 18 months of age. This may be due to the fact that HR-ASD participants who experienced symptoms at this age (EOA participants) were too few (n = 4) to drive a statistically significant difference. A significant association between age at scanning and discrete diagnosis outcome groups was observed with HR-TD being the oldest group and HR-non-TD the youngest one.

Table 1 Sample characteristics

		Groups according to diagnosis outcome			HR-ASD subgroups by age of first diagnosis	
	HR (n=20)	**HR-TD (n=8)**	**HR-nonTD (n=3)**	**HR-ASD (n=9)**	**LOA (n=5)**	**EOA (n=4)**
Age at scanning [months] (n = 20)	16.5 ± 1.6 (14.6 - 19.8)	17.7 ± 1.5 (15.6 - 19.8)	15.3 ± 0.5 (14.8 - 15.7)	15.8 ± 1.2 (14.6 - 18.3)**	15.2 ± 0.4 (14.6 - 15.7)	16.6 ± 1.4 (15.3 - 18.3)
Time interval between scans [months] (n = 20)	6.5 ± 0.9 (5.2 - 9.0)	6.8 ± 1.4 (5.2 - 9.0)	6.1 ± 0.5 (5.6 - 6.6)	6.3 ± 0.5 (5.6 - 7.2)	6.5 ± 0.5 (5.9 - 7.2)	6.1 ± 0.5 (5.6 - 6.5)
Gender [female percentage] (n = 20)	25%	37.5%	33.3%	11.1%	0%	25%
Age at 1st clinical assessment (n = 19)	18.1 ± 0.4 (17.6 - 19.1)	18.1 ± 0.4 (17.7 - 18.6)	17.8 ± 0.2 (17.6 - 18)	18.2 ± 0.4 (17.7 - 19.1)	18.4 ± 0.4 (17.7 - 19.1)	18 ± 0.1 (17.9 - 18.2)
ADOS CSS (n = 19)	3.5 ± 2.7 (1 - 10)	2.6 ± 2.1 (1 - 7)	2 ± 1 (1 - 3)	4.8 ± 3.1 (1 - 10)	2.4 ± 1.1 (1 - 4)	7.8 ± 1.7 (6 - 10)***
DQ (n = 19)	87.1 ± 14.2 (54.1 - 119.4)	96.4 ± 14.9 (87.3 - 119.4)	85.8 ± 11.8 (72.6 - 95.5)	80.4 ± 11.2 (54.1 - 90.9)	86.2 ± 5.1 (78.8 - 89.9)	73.2 ± 13.1 (54.1 - 83.2)
Age at 3rd clinical assessment (n = 20)	36.5 ± 1.2 (34.9 - 39.9)	36.9 ± 1.4 (35.6 - 39.9)	35.7 ± 0.7 (35.3 - 36.6)	36.9 ± 1.4 (34.9 - 38.3)	36 ± 0.8 (34.9 - 36.8)	36.8 ± 1.2 (35.5 - 38.3)
ADOS CSS (n = 20)	3.9 ± 2.6 (1 - 8)	1.5 ± 0.5 (1 - 2)	2.7 ± 1.5 (1 - 4)	6.3 ± 1.3 (5 - 9)****	6.4 ± 1.5 (5 - 9)	6.25 ± 1.3 (5 - 8)
DQ (n = 20)	87.5 ± 19.1 (70.8 - 108.0)	103.2 ± 5.3 (93.3 - 109.9)	76 ± 0.2 (75.9 - 76.3)	77.4 ± 20.8 (32.5 - 103.2)**	77.6 ± 28.9 (32.5 - 103.2)	77.1 ± 6.1 (70.8 - 84.6)

*Note: Statistical comparisons between groups: age at scanning p = 0.01 (one-way ANOVA) ; time interval between scans p = 0.47 (1-way ANOVA) ; Gender p = 0.43 (chi-square test) ; ADOS CSS at 18-mo p=0.16 (one-way ANOVA) ; DQ at 18-mo p=0.7 (one-way ANOVA) ; ADOS CSS at 36-mo p<0.0001 (one-way ANOVA) ; DQ at 36-mo p=0.0042 (one-way ANOVA). Statistical comparison between HR-ASD subgroups (LOA and EOA): age at scanning p=0.19 (Mann-Whitney U test) ; time interval between scans p=0.27 (Student T test) ; gender p=0.24 (chi-square test); ADOS CSS at 18-mo p=0.0008 (Student T test) ; DQ at 18-mo p=0.078 (Student T-test) ; ADOS CSS at 36-mo p=0.88 (Student T-test) ; DQ at 36-mo p=0.97 (Mann-Whitney U test). * p < 0.05 ; ** p < 0.01 ; *** p < 0.001 ; **** p < 0.0001.*

GWC rate of change increases globally in HR with typical development between age 1 and 2

In HR children who demonstrated typical development at age 3 (HR-TD), GWC was significantly correlated with time in almost all regions (Fig. 2A and supplementary material S1). The highest rates of change were found bilaterally in prefrontal areas, temporal poles and temporo-parietal junctions. Areas with the smallest rates of change were found in lateral and medial occipital lobes bilaterally, right paracentral gyrus, right insula, left subgenual region and left inferior frontal gyrus. No region exhibited a significantly decreasing GWC rate of change. There was no global difference between right and left hemisphere (Fig. 2B).

Increased GWC at 1.5 years old predicts ASD at age 3

A significant increase in mean GWC values in HR-ASD compared to HR-TD was found in the right IFG, right posterior middle temporal gyrus, right temporo-parietal junction, left inferior frontal gyrus and left middle temporal gyrus (Fig. 3). No regions displayed a significant decrease in mean GWC in HR-ASD compared to HR-TD (Table 2).

Table 2 Clusters of significant association between GWC and clinical outcomes

							LOA vs HR-TD		EOA vs HR-TD	
Mean GWC	**Cluster number**	**Anatomical Label**	**Size [mm^2]**	**CWP**	**Pvm**	**Effect size**	**pValue**	**Effect size**	**pValue**	**Effect size**
18 months ADOS CSS	1	right superior temporal sulcus	675.83	**0.04790**	3.721	0.64	0.3494	0.08791	**0.0284***	0.4302
	2	right lateral occipital	727.99	**0.03390**	2.411	0.43	0.96	0.000264	0.0962	0.2771
	3	left fusiform	732.40	**0.02630**	2.313	0.61	0.1395 (W)	0.275	**0.0151***	0.4993
	4	left pars opercularis	1149.28	**0.00100**	2.919	0.51	0.6705	0.01885	**0.0499***	0.3628
	5	left middle temporal	679.73	**0.04170**	3.121	0.46	0.3594 (W)	0.1187	0.0669	0.3253
36 months ADOS CSS	1	right inferior parietal	744.17	**0.02940**	3.560	0.43	0.0914	0.2372	**0.0132***	0.4745
	2	right precentral	750.59	**0.02810**	2.687	0.39	0.0914	0.2372	**0.0132***	0.4745
	3	right precuneus	877.68	**0.00970**	4.918	0.38	0.2526	0.117	**0.0371***	0.3661
	4	right lateral occipical	944.15	**0.00530**	2.062	0.19	0.9829	4.37E-05	0.0981	0.2497
	5	left middle temporal	716.61	**0.03090**	2.897	0.48	**0.0229***	0.3884	0**.0066****	0.5388
	6	left superior parietal	1141.39	**0.00100**	2.908	0.23	0.2421	0.122	0.2923 (W)	0.3042
Diagnosis outcome (HR-TD *vs* HR-ASD)	1	right supramarginal	846.86	**0.01210**	3.267	0.32	0.0890	0.2403	**0.0302***	0.389
	2	right inferior parietal	1033.13	**0.00250**	3.892	0.28	0.1528	0.1766	**0.0122***	0.4827
	3	right rostral middle frontal	1712.40	**0.00010**	3.050	0.15	0.5820 (W)	0.03508	**0.0433***	0.3486
	4	left middle temporal	1031.10	**0.00210**	3.942	0.46	**0.0341***	0.3472	**0.0025****	0.6148
	5	left pars opercularis	798.22	**0.01510**	5.042	0.19	0.2931 (W)	0.12	**0.0471***	0.3386

	6	left pars orbitalis	2530.44	**0.00010**	4.400	0.11	0.8326 (W)	0.005501	0.0573	0.3157
ΔGWC										
18 months ADOS CSS	1	right superior parietal	760.54	**-0.02620**	-2.971	-0.50	-0.8372	-0.004428	-0.0917	-0.2835
	2	right pars opercularis	4235.26	**-0.00010**	-3.782	-0.48	-0.2653	-0.1222	-0.0925	-0.2824
	3	right inferior parietal	1098.39	**-0.00150**	-2.909	-0.48	-0.6099	-0.02699	**-0.0454***	-0.3745
	4	right transverse temporal	807.11	**-0.01820**	-3.209	-0.43	-0.4153	-0.06736	-0.0692	-0.3209
	5	left precuneus	890.95	**-0.00720**	-5.256	-0.72	-0.2984	-0.1074	**-0.0421***	-0.3838
	6	left supramarginal	1720.35	**-0.00010**	-3.462	-0.62	-0.6361	-0.02326	-0.0712	-0.3172
	7	left frontal superior	3451.95	**-0.00010**	-4.219	-0.60	-0.4641	-0.05476	**-0.0224***	-0.4567
	8	left frontal superior	1854.61	**-0.00010**	-4.591	-0.53	-0.3103	-0.1025	-0.0781	-0.305
	9	left superior parietal	663.22	**-0.04690**	-3.734	-0.52	-0.3799	-0.07784	-0.2923 (W)	-0.3042
	10	left middle temporal	1105.22	**-0.00120**	-3.066	-0.51	-0.0903	-0.2601	-0.0576	-0.3446
Mean CT										
Diagnosis outcome (HR-TD *vs* HR-ASD)	1	left frontal superior	805.5	**-0.01245**	-2.191	-0.22	-0.3481	-0.08	**-0.0225***	-0.42

Note: Detailed results of surface-based statistical analyses. Cluster numbers refer to numbers displayed in figures 3, 4 and 5 and are listed in order of decreasing effect size within each analysis. Anatomical labels refer to location of vertex with maximal p-value (Pvm) according to FreeSurfer Desikan parcellation atlas. Pvm are reported in T-stat values which is equal to -log(p-value). For post-hoc analyses, a (W) indicates if a non-parametric distribution was detected and subsequently Mann-Whitney U test was used instead of Student T-test. Effect sizes are expressed with either Cohen's d or R squared (r2) values. * $p < 0.05$; ** $p < 0.01$.

ASD symptom severity at 18 and 36 months is associated with mean GWC between 12–24 months of age

Mean GWC was positively correlated with autism symptom severity (ADOS CSS) at 18-months in right superior temporal sulcus, right posterior fusiform gyrus, left posterior fusiform gyrus, left insula, left inferior frontal gyrus

and left middle temporal gyrus (Fig. 4A). Mean GWC was also positively correlated with autism symptom severity at age 3 (36-months ADOS CSS), but in different regions, including the right posterior part of middle temporal gyrus, right inferior part of precentral gyrus, right precuneus, right lateral occipital gyrus, left middle temporal gyrus and left lateral occipital gyrus (Fig. 4B) (Table 2). All clusters are illustrated in supplementary material S2.

Slower GWC rate of change between age 12 and 24 months is exclusively associated with symptom severity at 18 months

A negative correlation between symptom severity (ADOS CSS) at 18-mo and ΔGWC values was observed in the right parietal posterior region, right dorsolateral prefrontal region, right temporo-parietal junction, left temporo-parietal junction, left medial part of the superior frontal gyrus, left posterior parietal cortex and left middle temporal gyrus (Fig. 5A). Later symptom severity (36-mo ADOS CSS) as well as diagnosis group comparison (HR-TD *vs* HR-ASD) were not associated with any significant differences in ΔGWC between age 1 and 2. See Table 2 and supplementary material S3 for detailed results and illustrations.

Alterations in GWC values are influenced by age of first ASD-related symptoms onset

Post hoc analyses of HR-ASD subgroups based on whether autism symptoms emerged prior to (EOA) or after (LOA) 18 months reveal a significant effect of early symptom onset. In clusters with higher mean GWC values in HR-TD compared to HR-ASD the EOA subgroup exhibited increased mean GWC values compared to HR-TD in all clusters except from left inferior frontal gyrus. The LOA subgroup exhibited increased mean GWC values compared to HR-TD only in the left middle temporal gyrus cluster (Fig. 3).

For clusters with significant correlation between mean GWC and symptom severity at 18-months, there were significant differences in mean GWC between EOA and HR-TD in right superior temporal sulcus, left posterior fusiform gyrus and left inferior frontal gyrus. There was no difference in mean GWC between LOA and HR-TD (Fig. 4A and supplementary material S2). For clusters with significant correlation between mean GWC and 36 months symptom severity (36-mo ADOS CSS), we found significant differences in mean GWC between EOA and HR-TD in the right posterior part of the middle temporal gyrus, right inferior part of the precentral gyrus, right precuneus and left middle temporal gyrus. For the same clusters, we only found significant differences between LOA and HR-TD in left middle temporal gyrus (Fig. 4B and supplementary material S2).

For clusters with significant correlation between symptom severity at time of scan and ΔGWC significant differences were found in ΔGWC between EOA and HR-TD in the right temporo-parietal junction, left precuneus and the posterior part of the superior frontal gyrus. There was no difference between HR-TD and LOA in any of the clusters (Fig. 5 and supplementary material S3). All results of post-hoc analyses between EOA/LOA and HR-TD are reported in Table 2.

Cortical thickness at 12–24 months is decreased in medial superior frontal gyrus in the HR-ASD group

We found decreased mean CT values in HR-ASD compared to HR-TD in a single cluster located in the medial part of the superior frontal gyrus (Suppl. Material S4). Apart from this cluster, no differences in ΔCT between HR-ASD and HR-TD were observed. There was also no effect of symptom severity (either 18-months or 36-months ADOS CSS) on longitudinal CT parameters (mean CT and ΔCT). See Table 2 for detailed results.

Discussion

Our aim was to use structural MRI to conduct an exploratory surface-based analysis to determine if alterations in tissue contrast across the gray-white matter boundary in toddlers at high-risk for ASD could represent an early biomarker of clinical outcome (i.e., autism diagnosis) at age 3 and whether alterations in GWC are associated with autism symptom severity. Firstly, HR children with typical development were found to exhibit widespread increases of GWC values with time from ages 12 to 24 months. This result provides a first normative reference for typical GWC values at this age in HR toddlers. Secondly, ASD outcome at 3 years of age was associated with widespread (though well localized) increased GWC values during the second year of life compared to HR infants with a TD outcome. These results suggest that brain microstructural alterations in ASD are already well-established at the end of infancy and are associated with clinical outcomes later in development. Lastly, individuals who experienced earlier onset of ASD symptoms (i.e. at 18 months of age) had a distinct neurobiological signature characterized by a slower rate of change in GWC between 12 and 24 months of age and globally stronger alterations in all GWC values compared to TD.

Typical development in a HR population is characterized by increasing GWC values between age 1 and 2

The only previous study exploring GWC changes in TD across the same age range as the current study also identified brain regions where GWC values increased between age 12 and 19 months (28). Clusters found by Travis *et al* correspond to regions observed in the current study with the highest ΔGWC values in the HR-TD group (left dorso-lateral prefrontal cortex and left anterior temporal lobe). However, Travis *et al* found more focal regions with significant increases in ΔGWC in comparison to our results and all their findings were exclusively localized in the left hemisphere. Several possible explanations may explain these differences. One is the exploration of a shorter age interval by Travis *et al.* (from 12 to 19 months instead of 12 to 24 months in our study) which may result in reduced effects of time on GWC. Another explanation is the more conservative method to correct for multiple corrections used by Travis *et al.* (false discovery rate instead of MCS). Nonetheless, collectively these results converge in supporting the idea that GWC tends to increase with time in various regions during the second year of life in TD.

Relations between our results and GWC alterations previously found at older ages

Considering existing literature exploring GWC in ASD, GWC differences in regions reported as altered in older populations with ASD were also observed in the current study. For instance, bilateral middle temporal gyri (MTG) and bilateral fusiform gyri (FG) exhibited decreased GWC in Andrews *et al* (24). Furthermore, right precuneus, right occipital gyri, right FG and left inferior frontal gyrus (IFG) exhibited decreased GWC values in association with ASD from late childhood to early adulthood in Mann *et al.* (25). Although brain regions indicated by the current study are consistent with these two previous studies of adults, we found that ASD was associated with increased GWC. Although inconsistent, these observations are not necessarily incompatible. One potential explanation is the possibility that between the age explored in our study (i.e. before two years of age), late childhood and adulthood a global decrease of GWC rate of change occurs amongst children with ASD. This hypothesis is supported by our finding that the second year of life is characterized by slower GWC rates of change in individuals who experienced ASD-related symptoms during the period of scan acquisitions. Further studies exploring GWC trajectories after the age of two are needed to determine if all ASD phenotypes undergo a diffuse slowdown in GWC rate of change at some point.

Some of our results were consistent in location and in direction with previous literature, e.g. increased GWC in bilateral occipital gyri was previously described by Fouquet *et al.* in adults with ASD (26). This result suggests that increased GWC in the visual cortex remains higher across lifespan in individuals with ASD compared to TD. Also, the regions that we found undergoing slower GWC changes with time (ΔGWC) were consistent with areas described to have later decreased GWC in Mann *et al.* (for bilateral prefrontal and parietal posterior cortice) and Andrews *et al.* (for left MTG, left precuneus and left medial part of superior frontal gyrus).

Increased GWC at 12–24 months of age relates to ASD outcome at 36 months of age

Areas in which increased mean GWC s were associated with ASD diagnosis at age 3 (Fig. 3) have all been previously implicated in functions altered in ASD, including language and social processing (45). Left middle temporal gyrus (MTG) and left inferior frontal gyrus (IFG), for instance, are both implicated in semantic processing which is one of the most commonly found altered domains of language in ASD (46) (47) (48). Moreover, left IFG is known to be functionally altered during semantic processing tasks in adults with ASD (49). Left MTG and left IFG both exhibit morphometric alterations in adults with ASD (50). Right MTG has shown metabolic activation related to multimodal integration of communication cues (i.e. gaze, speech and gesture) (51) in TD, processes known to be challenging for individuals with ASD (52).

Regarding regions in which high mean GWC values at age 12–24 months were associated with symptom severity at age 3 (Fig. 4B), some overlap with clusters associated with later diagnosis outcomes are present, such as left IFG, left MTG and right MTG. Nonetheless, some clusters were exclusively associated with symptom severity at age 3 and not later diagnosis outcome. This is the case for the right precuneus, a key component of the default mode network (DMN), which is implicated in mentalizing (i.e. building inferences about others' mental states). Such "theory of mind" deficits have been highlighted as a feature of ASD for decades (53) and there is growing evidence supporting the presence of alterations in the DMN and more specifically precuneus in ASD (54). Increased mean GWC values in primary cortices such as the occipital gyri (visual) and precentral gyrus (motor) are consistent with results on GWC in adults with ASD reported by *Fouquet et al.* (26). It is also consistent with previous reports of disruption of primary motor area organization in children with ASD (55) as well as functional and structural alterations in occipital regions in the same population (56). Our results suggest that a common microstructural mechanism during the first years of life could be at play across various cortical areas that all have been independently reported as functionally and/or structurally altered in ASD.

Finally, regions exhibiting increased mean GWC values in relation to symptom severity at 18-months (Fig. 4A) are mostly overlapping with regions that are associated with later ASD diagnoses (IFG, left and right MTG). However, altered GWC values in bilateral fusiform gyri (FG) are only associated with early onset of symptoms and not with later ASD onset. The FG is implicated in face and object identification and has also been reported as having altered morphologic development in ASD (57). Thus, alterations of FG may result in earlier onset of symptoms since face identification is part of the first prerequisite for the development of social interactions (58).

Slower GWC rate of change between 12 and 24 months of age as a neural signature of the onset of ASD symptoms at the age of 18 months or earlier

A widespread decrease in the rate of GWC change between 12 and 24 months of age was associated with ASD symptom severity at 18 months. Most clusters with slower ΔGWC did not overlap with regions with increased mean GWC associated with diagnostic outcome at age 3 described above (Fig. 5B). ΔGWC alterations were

largely localized within the central executive network (CEN), including bilateral dorso-lateral prefrontal and bilateral posterior parietal cortex (59). Functional alterations of CEN have previously been reported in ASD (60). Decreased GWC rate of change was also observed in left temporo-parietal junction (TPJ), left precuneus and left middle temporal gyrus (MTG). Left TPJ and left precuneus both belong to the DMN which has been found altered in ASD (54). Left MTG is the only region exhibiting both an increased mean GWC along with a decreased ΔGWC between age 12 and 24 months. This alteration of the left MTG microstructure further supports its possible role as a key region in the early development of various phenotypes of ASD. Overall, these results suggest that participants who manifest very early symptoms of ASD are characterized by a specific pattern of dynamic GWC changes during the second year of life, largely affecting regions implicated in executive functions.

Neurobiological Interpretations Of Altered GWC Values

To understand the neurobiological correlates to our findings, an important step would be to explore if GWC differences result from alterations in cortical grey matter, superficial white matter, or a combination of both structures. Since GWC measures depend on two parameters (WM intensity and GM intensity), changes in GWC values can be caused either by changes in one or both of these variables. The GWC measure is proportional to WM intensity and inversely proportional to GM intensity. In other words, a darker grey matter intensity and a brighter superficial white matter intensity would both result in increased GWC values. The opposite reasoning holds for explaining decreased GWC values. Unfortunately, in qualitative MRI techniques such as T1-weighted scans, the absolute intensity values can be influenced by many factors (type of setup, detectors used, *etc.*) resulting in great intra- and inter-participants variability (61). It is thus of limited utility to perform statistical analyses on GM and/or WM intensities *per se*, an issue that was already highlighted in early studies using GWC (43).

Despite this intrinsic limitation, we can speculate here on the likelihood of various neurobiological correlates which could explain enhanced GWC values during the second year of life. First, increased GWC could result from decreased GM intensity (i.e. a darker cortical gray matter on T1w images). Many studies have highlighted alterations of cortical cytoarchitecture in ASD which could lead to alterations in GM intensity. For instance, greater density of dendritic spines of pyramidal cells as well as an increased neural density have been reported in various cortical regions and in the amygdala amongst children and adults with ASD (62). Evidence suggests that an increased number of minicolumns (which constitute the basic structural units of cortical architecture) could be a potential cause of neural excess in ASD (63). If our results are explained by increased neural density at the end of infancy they would thus bring further support to the hypothesis that ASD is characterized by altered neural proliferation, migration and lamination processes (27). Another explanation for decreased GM intensity would be a delay in intracortical myelination, a mechanism that was already suggested by Fouquet *et al.* (26). Nevertheless, deficits in intracortical myelin are not as well documented in ASD and limited to animal model studies (64).

Increased WM intensity represents an alternative (although not exclusive) explanation to increased GWC. If this were the case, increased myelination would be a likely contributor, since myelin is the most determinant contribution to WM intensity (65). Early increased myelination in ASD has been suggested by several independent studies exploring deep white matter tracts in infancy using diffusion weighted imaging making this hypothesis plausible (66)(67)(20)(19). If true, these results would support the idea that ASD is characterized by

an increased myelination process which is not limited to deep WM but rather generalized to all WM during the first months of life.

Potential mechanisms underlying a decreased GWC rate of change include faster increases in GM intensity (i.e. cortical gray matter becoming rapidly brighter) and/or slower increases in WM intensity (i.e. superficial white matter becoming slowly brighter). Slower WM intensity changes could be explained by a delay in myelination of superficial WM. This hypothesis would be consistent with previous reports of decreased myelin in superficial WM in adolescent and adults with ASD (68). Furthermore, this hypothesis would converge with Wolff *et al*. who showed an early developmental pattern consisting of increased myelin content in various deep WM tracts during infancy followed by a delay in myelination process after age 1 in ASD compared to TD (19).

GWC alterations as a specific neurobiological signature of onset of ASD symptoms prior to 18 months of age

The current findings indicate that differences in GWC are related to age at which first ASD symptoms occur. First, symptom severity at 18 months (i.e. ADOS CSS at 18 months) was associated with a pattern of GWC alterations that was distinct from the pattern of alterations associated with s of later clinical outcome (ADOS CSS and diagnosis outcome at 36 months). Symptom severity at 18 months was specifically correlated with increased GWC in bilateral FG. Moreover, slower GWC rates of change were specifically observed in relation to symptom severity at time of scan and were not linked to any later clinical outcome. Second, the subset of HR-ASD with established diagnosis at 18 months (i.e. early onset autism) exhibited the greatest magnitude in GWC alterations within all clusters across all analyses compared to HR-ASD with a later onset of ASD after 18 months (Supplementary material S2, S3 and S4). Since the early and late onset subgroups did not exhibit any difference in either symptom severity or global development (DQ) at age 3 (see Table 1), these differences can solely be explained by age of first symptom onset and not by later symptom severity or cognitive level. Together, these results suggest that ASD with an onset of symptoms prior to 18 months is characterized by a specific pattern of early GWC alterations at the age of 1–2 years which consists of enhanced GWC in bilateral FG, widespread slower GWC rate of change and a trend for all GWC

Limitations And Further Perspectives

Some limitations to our study need to be highlighted. First is the small size of our sample. This is, however, the first study examining GWC at the age when autism symptoms emerge. The overall consistency in the direction of alteration of GWC across regions and convergence in the location of altered areas compared to previous literature support the validity of our results. Still, replication with larger samples is necessary, especially to better delineate different phenotypic subgroups according to their distinct GWC alterations. Second, the different outcome subgroups had slight but statistically significant differences in age at scanning. One could argue that this age difference could influence the differences in GWC values. However, it should be noted that age at scanning was regressed as a nuisance factor to limit its confounding effect and HR-TD was the oldest group of the sample. Also, our results and others (28) suggest that GWC is increasing with age during the second year of life in TD. Thus, if our results were driven by age differences between groups, an opposite direction would be expected in our group analyses (i.e. increased mean GWC in HR-TD who are older compared to HR-ASD who are younger). Another possible limitation to this study is the potential confounding factor of cortical thickness alterations (43). Vertex-wise analyses only revealed a single focal cluster with decreased mean cortical thickness in the HR-ASD group. The majority of regions found to have altered GWC values in relation to ASD showed no

significant differences in cortical thickness. To overcome limitations in the biological interpretation of GWC measures, future studies would benefit from implementing MRI techniques that offer a quantitative measure of the local intensity to decipher respective contributions of cortical grey matter and superficial white matter to GWC alterations. One solution could be the use of imaging methods that precisely “map” the physical T1 or T2 properties of the tissue to allow local quantification and inter-participants comparison of microstructure content (69)(70).

Conclusion

In conclusion, our results support the hypothesis that ASD is associated with widespread microstructural alterations at the gray-white matter boundary during the first two years of life. These alterations were linked to symptom severity at 18 months of age , and also with later diagnosis outcomes and symptom severity at 3 years of age. GWC alterations in ASD consisted of increased contrast across many brain regions relevant for social processing, language acquisition and primary visual and motor cortical regions. In general, GWC alterations were stronger in toddlers who exhibited ASD-related symptoms at 18 months compared to those who developed ASD after 18 months. Moreover, compared to participants with later symptom onset, those who already experienced ASD-related symptoms at 18 months of age exhibited slower GWC rates of change during the second year of life in many regions that are important for attentional and executive processing. A potential neurobiological explanation of this finding might involve delayed myelination of superficial white matter, a hypothesis which will need to be assessed by further quantitative neuroimaging studies. Together, our results suggest that onset of ASD-related symptoms prior to 18 months could be an independent clinical phenotype with a specific corresponding developmental brain signature.

Abbreviations

ADOS: Autism Diagnostic Observation Schedule; ASD: Autism Spectrum Disorder; CEN: central executive network; CSS: calibrated severity score; CT: Cortical thickness; CWP: Cluster-wise p-value; DMN: default mode network; DQ: Developmental quotient; EOA: Early onset ASD; FG: Fusiform gyri; FWHM: Full-width at half-maximum; GLM: General linear model; GM: Gray matter; GWC: Gray-white matter contrast; HR: High risk for ASD; HR-non-TD: HR with atypical development; HR-TD: HR with TD; IFG: Inferior frontal gyrus; LOA: Late onset ASD; MCS: Monte-Carlo simulation; mGWC: mean GWC; MRI: Magnetic resonance imaging; MSEL: Mullen Scales of Early Learning; MTG: Middle temporal gyrus; Pvm: vertex with maximal p-value; SPC: Symmetrical percentage of change; TD: Typical development; TPJ: temporo-parietal junction; WM: White matter; ΔCT: CT rate of change; ΔGWC: GWC rate of change.

Declarations

Funding

This research was supported by the Swiss National Foundation Synapsy Grant No. (51NF40 – 185897) and the Swiss National Foundation for Scientific Research Grant (No. 323630-191227 to M.G., and #163859 & #190084 to M.S.). This work was also supported by the National Institutes of Health (R01MH068398 to S.O., R01MH104438 to C.W.N., R01MH103284 to M.S. and R01MH103371 to D.G.A.) and the University of California (UC) Davis MIND Institute. The MIND Institute Intellectual and Developmental Disabilities Research Center

(U54HD079125) and the Autism Center of Excellence (P50 HD093079) awarded by the National Institute of Child Health and Development (NICHD) also supported this project. D.S.A. is supported by the MIND Institute Autism Research Training Program (T32MH073124).

Authors' contributions

S.O., D.G.A., C.W.N. conceived of and designed the study and acquired all clinical and neuroimaging data. D.S.A., J.K.L., and G.S.Y. provided tehchnical assistance. M.G. prepared and analyzed the data under the supervision of M.S. and C.W.N. All authors participated in interpretation of results. M.G. wrote the manuscript with the input from the all other authors. All authors read and approved the final manuscript.

Availability of data and materials

The datasets generated in the current study are available from the corresponding author on reasonable request.

Ethics approval and consent to participate

All participants gave informed written consent in accordance with the ethics approval by the University of California at Davis Institutional Review Board.

Consent for publication

Not applicable.

Competing interests

The authors have no competing interests to report.

References

1. American Psychiatric Association. Diagnostic and Statistical Manual of Mental Disorders [Internet]. Fifth Edition. American Psychiatric Association; 2013 [cited 2018 Nov 4]. Available from: https://psychiatryonline.org/doi/book/10.1176/appi.books.9780890425596
2. Lai M-C, Lombardo MV, Baron-Cohen S. Autism. The Lancet. 2014 Mar 8;383(9920):896–910.
3. Baio J, Wiggins L, Christensen DL, Maenner MJ, Daniels J, Warren Z, et al. Prevalence of Autism Spectrum Disorder Among Children Aged 8 Years — Autism and Developmental Disabilities Monitoring Network, 11 Sites, United States, 2014. MMWR Surveill Summ. 2018 Apr 27;67(6):1–23.
4. Weintraub K. The prevalence puzzle: Autism counts. Nature. 2011 Nov;479(7371):22–4.
5. Huguet G, Ey E, Bourgeron T. The Genetic Landscapes of Autism Spectrum Disorders. Annu Rev Genom Hum Genet. 2013 Aug 31;14(1):191–213.
6. Reichow B. Overview of meta-analyses on early intensive behavioral intervention for young children with autism spectrum disorders. J Autism Dev Disord. 2012 Apr;42(4):512–20.
7. Brett D, Warnell F, McConachie H, Parr JR. Factors Affecting Age at ASD Diagnosis in UK: No Evidence that Diagnosis Age has Decreased Between 2004 and 2014. J Autism Dev Disord. 2016;46(6):1974–84.

8. Daniels AM, Halladay AK, Shih A, Elder LM, Dawson G. Approaches to enhancing the early detection of autism spectrum disorders: a systematic review of the literature. J Am Acad Child Adolesc Psychiatry. 2014 Feb;53(2):141–52.
9. Howlin P, Magiati I, Charman T. Systematic Review of Early Intensive Behavioral Interventions for Children With Autism. MacLean, Jr. WE, editor. American Journal on Intellectual and Developmental Disabilities. 2009 Jan 1;114(1):23–41.
10. Ozonoff S, Young GS, Carter A, Messinger D, Yirmiya N, Zwaigenbaum L, et al. Recurrence risk for autism spectrum disorders: a Baby Siblings Research Consortium study. Pediatrics. 2011 Sep;128(3):e488-495.
11. Szatmari P, Chawarska K, Dawson G, Georgiades S, Landa R, Lord C, et al. Prospective Longitudinal Studies of Infant Siblings of Children With Autism: Lessons Learned and Future Directions. J Am Acad Child Adolesc Psychiatry. 2016 Mar;55(3):179–87.
12. Sacrey L-AR, Zwaigenbaum L, Bryson S, Brian J, Smith IM, Roberts W, et al. Parent and clinician agreement regarding early behavioral signs in 12- and 18-month-old infants at-risk of autism spectrum disorder: Parent and clinician agreement in autism. Autism Research. 2018 Mar;11(3):539–47.
13. Sacrey L-AR, Zwaigenbaum L, Bryson S, Brian J, Smith IM, Roberts W, et al. Screening for Behavioral Signs of Autism Spectrum Disorder in 9-Month-Old Infant Siblings. J Autism Dev Disord [Internet]. 2020 Jan 14 [cited 2020 Jan 30]; Available from: http://link.springer.com/10.1007/s10803-020-04371-0
14. Ozonoff S, Young GS, Landa RJ, Brian J, Bryson S, Charman T, et al. Diagnostic stability in young children at risk for autism spectrum disorder: a baby siblings research consortium study. J Child Psychol Psychiatr. 2015 Sep;56(9):988–98.
15. Wolff JJ, Jacob S, Elison JT. The journey to autism: Insights from neuroimaging studies of infants and toddlers. Dev Psychopathol. 2018 May;30(2):479–95.
16. Shen MD, Nordahl CW, Young GS, Wootton-Gorges SL, Lee A, Liston SE, et al. Early brain enlargement and elevated extra-axial fluid in infants who develop autism spectrum disorder. Brain. 2013 Sep;136(Pt 9):2825–35.
17. Shen MD, Kim SH, McKinstry RC, Gu H, Hazlett HC, Nordahl CW, et al. Increased Extra-axial Cerebrospinal Fluid in High-Risk Infants who Later Develop Autism. Biol Psychiatry. 2017 Aug 1;82(3):186–93.
18. The IBIS Network, Hazlett HC, Gu H, Munsell BC, Kim SH, Styner M, et al. Early brain development in infants at high risk for autism spectrum disorder. Nature. 2017 Feb;542(7641):348–51.
19. Wolff JJ, Gu H, Gerig G, Elison JT, Styner M, Gouttard S, et al. Differences in White Matter Fiber Tract Development Present From 6 to 24 Months in Infants With Autism. AJP. 2012 Jun;169(6):589–600.
20. Wolff JJ, Gerig G, Lewis JD, Soda T, Styner MA, Vachet C, et al. Altered corpus callosum morphology associated with autism over the first 2 years of life. Brain. 2015 Jul;138(7):2046–58.
21. Avino TA, Hutsler JJ. Abnormal cell patterning at the cortical gray–white matter boundary in autism spectrum disorders. Brain Research. 2010 Nov;1360:138–46.
22. Salat DH, Lee SY, van der Kouwe AJ, Greve DN, Fischl B, Rosas HD. Age-associated alterations in cortical gray and white matter signal intensity and gray to white matter contrast. Neuroimage. 2009 Oct 15;48(1):21–8.
23. for the Alzheimer's Disease Neuroimaging Initiative, Jefferson AL, Gifford KA, Damon S, Chapman GW, Liu D, et al. Gray & white matter tissue contrast differentiates Mild Cognitive Impairment converters from non-

converters. Brain Imaging and Behavior. 2015 Jun;9(2):141–8.

24. Andrews DS, Avino TA, Gudbrandsen M, Daly E, Marquand A, Murphy CM, et al. In Vivo Evidence of Reduced Integrity of the Gray–White Matter Boundary in Autism Spectrum Disorder. Cereb Cortex. 2017 Feb;27(2):877–87.
25. MRC AIMS Consortium, Mann C, Bletsch A, Andrews D, Daly E, Murphy C, et al. The effect of age on vertex-based measures of the grey-white matter tissue contrast in autism spectrum disorder. Molecular Autism. 2018 Dec;9(1):49.
26. Fouquet M, Traut N, Beggiato A, Delorme R, Bourgeron T, Toro R. Increased contrast of the grey-white matter boundary in the motor, visual and auditory areas in Autism Spectrum Disorders [Internet]. Neuroscience; 2019 Sep [cited 2020 Mar 23]. Available from: http://biorxiv.org/lookup/doi/10.1101/750117
27. Packer A. Neocortical neurogenesis and the etiology of autism spectrum disorder. Neuroscience & Biobehavioral Reviews. 2016 May;64:185–95.
28. Travis KE, Curran MM, Torres C, Leonard MK, Brown TT, Dale AM, et al. Age-related Changes in Tissue Signal Properties Within Cortical Areas Important for Word Understanding in 12- to 19-Month-Old Infants. Cerebral Cortex. 2014 Jul;24(7):1948–55.
29. Ozonoff S, Iosif A-M, Baguio F, Cook IC, Hill MM, Hutman T, et al. A Prospective Study of the Emergence of Early Behavioral Signs of Autism. Journal of the American Academy of Child & Adolescent Psychiatry. 2010 Mar;49(3):256-266.e2.
30. Mullen EM. Mullen scales of early learning. Circle Pines, MN: American Guidance Service; 1995.
31. Lord C, Risi S, DiLavore PS, Shulman C, Thurm A, Pickles A. Autism From 2 to 9 Years of Age. Arch Gen Psychiatry. 2006 Jun 1;63(6):694.
32. Lord C, Rutter M, DiLavore P, Risi S. Autism diagnostic observation schedule: generic. Los Angeles: Western Psychological Services; 2002.
33. Gotham K, Pickles A, Lord C. Standardizing ADOS Scores for a Measure of Severity in Autism Spectrum Disorders. J Autism Dev Disord. 2009 May;39(5):693–705.
34. Rutter M, DiLavore PC, Risi S, Gotham K, ishop S. Autism diagnostic observation schedule: ADOS-2. Torrance, CA: Western Psychological Services.; 2012.
35. American Psychiatric Association (APA). Diagnostic and statistical manual of mental disorders (text revision). 4th edn. Washington, DC: APA; 2000.
36. Nordahl CW, Simon TJ, Zierhut C, Solomon M, Rogers SJ, Amaral DG. Brief report: methods for acquiring structural MRI data in very young children with autism without the use of sedation. J Autism Dev Disord. 2008 Sep;38(8):1581–90.
37. Nordahl CW. Increased Rate of Amygdala Growth in Children Aged 2 to 4 Years With Autism Spectrum Disorders: A Longitudinal Study. Arch Gen Psychiatry. 2012 Jan 1;69(1):53.
38. Dale AM, Fischl B, Sereno MI. Cortical Surface-Based Analysis. NeuroImage. 1999 Feb;9(2):179–94.
39. Fischl B, Sereno MI, Dale AM. Cortical Surface-Based Analysis. NeuroImage. 1999 Feb;9(2):195–207.
40. Fischl B, Sereno MI, Tootell RB, Dale AM. High-resolution intersubject averaging and a coordinate system for the cortical surface. Hum Brain Mapp. 1999;8(4):272–84.
41. Fischl B, Dale AM. Measuring the thickness of the human cerebral cortex from magnetic resonance images. Proc Natl Acad Sci USA. 2000 Sep 26;97(20):11050–5.

42. Reuter M, Schmansky NJ, Rosas HD, Fischl B. Within-subject template estimation for unbiased longitudinal image analysis. NeuroImage. 2012 Jul;61(4):1402–18.
43. Westlye LT, Walhovd KB, Dale AM, Espeseth T, Reinvang I, Raz N, et al. Increased sensitivity to effects of normal aging and Alzheimer's disease on cortical thickness by adjustment for local variability in gray/white contrast: A multi-sample MRI study. NeuroImage. 2009 Oct;47(4):1545–57.
44. Hagler DJ, Saygin AP, Sereno MI. Smoothing and cluster thresholding for cortical surface-based group analysis of fMRI data. NeuroImage. 2006 Dec;33(4):1093–103.
45. Amaral DG, Schumann CM, Nordahl CW. Neuroanatomy of autism. Trends in Neurosciences. 2008 Mar;31(3):137–45.
46. Wei T, Liang X, He Y, Zang Y, Han Z, Caramazza A, et al. Predicting Conceptual Processing Capacity from Spontaneous Neuronal Activity of the Left Middle Temporal Gyrus. Journal of Neuroscience. 2012 Jan 11;32(2):481–9.
47. Tager-Flusberg H, Walenski M, Ullman M. Language in Autism. In: Moldin S, Rubenstein J, editors. Understanding Autism [Internet]. CRC Press; 2006 [cited 2020 Jun 26]. p. 175–203. Available from: http://www.crcnetbase.com/doi/10.1201/9781420004205.ch9
48. Huang J, Zhu Z, Zhang JX, Wu M, Chen H-C, Wang S. The role of left inferior frontal gyrus in explicit and implicit semantic processing. Brain Research. 2012 Feb;1440:56–64.
49. Harris GJ, Chabris CF, Clark J, Urban T, Aharon I, Steele S, et al. Brain activation during semantic processing in autism spectrum disorders via functional magnetic resonance imaging. Brain and Cognition. 2006 Jun;61(1):54–68.
50. Libero LE, DeRamus TP, Deshpande HD, Kana RK. Surface-based morphometry of the cortical architecture of autism spectrum disorders: volume, thickness, area, and gyrification. Neuropsychologia. 2014 Sep;62:1–10.
51. Holler J, Kokal I, Toni I, Hagoort P, Kelly SD, Özyürek A. Eye'm talking to you: speakers' gaze direction modulates co-speech gesture processing in the right MTG. Social Cognitive and Affective Neuroscience. 2015 Feb 1;10(2):255–61.
52. Stevenson RA, Siemann JK, Schneider BC, Eberly HE, Woynaroski TG, Camarata SM, et al. Multisensory Temporal Integration in Autism Spectrum Disorders. J Neurosci. 2014 Jan 15;34(3):691–7.
53. Baron-Cohen S, Leslie AM, Frith U. Does the autistic child have a "theory of mind"? Cognition. 1985 Oct;21(1):37–46.
54. Padmanabhan A, Lynch CJ, Schaer M, Menon V. The Default Mode Network in Autism. Biological Psychiatry: Cognitive Neuroscience and Neuroimaging. 2017 Sep;2(6):476–86.
55. Nebel MB, Joel SE, Muschelli J, Barber AD, Caffo BS, Pekar JJ, et al. Disruption of functional organization within the primary motor cortex in children with autism: Functional Parcellation of the Motor Cortex. Hum Brain Mapp. 2014 Feb;35(2):567–80.
56. Jung M, Tu Y, Lang CA, Ortiz A, Park J, Jorgenson K, et al. Decreased structural connectivity and resting-state brain activity in the lateral occipital cortex is associated with social communication deficits in boys with autism spectrum disorder. NeuroImage. 2019 Apr;190:205–12.
57. Dougherty CC, Evans DW, Katuwal GJ, Michael AM. Asymmetry of fusiform structure in autism spectrum disorder: trajectory and association with symptom severity. Molecular Autism. 2016 Dec;7(1):28.

58. Chevallier C, Kohls G, Troiani V, Brodkin ES, Schultz RT. The Social Motivation Theory of Autism. Trends Cogn Sci. 2012 Apr;16(4):231–9.
59. Fox MD, Corbetta M, Snyder AZ, Vincent JL, Raichle ME. Spontaneous neuronal activity distinguishes human dorsal and ventral attention systems. Proceedings of the National Academy of Sciences. 2006 Jun 27;103(26):10046–51.
60. Perez Velazquez JL, Barcelo F, Hung Y, Leshchenko Y, Nenadovic V, Belkas J, et al. Decreased brain coordinated activity in autism spectrum disorders during executive tasks: Reduced long-range synchronization in the fronto-parietal networks. International Journal of Psychophysiology. 2009 Sep;73(3):341–9.
61. Lutti A, Dick F, Sereno MI, Weiskopf N. Using high-resolution quantitative mapping of R1 as an index of cortical myelination. NeuroImage. 2014 Jun;93:176–88.
62. Avino TA, Barger N, Vargas MV, Carlson EL, Amaral DG, Bauman MD, et al. Neuron numbers increase in the human amygdala from birth to adulthood, but not in autism. Proc Natl Acad Sci USA. 2018 Apr 3;115(14):3710–5.
63. Casanova MF, van Kooten IAJ, Switala AE, van Engeland H, Heinsen H, Steinbusch HWM, et al. Minicolumnar abnormalities in autism. Acta Neuropathol. 2006 Sep;112(3):287–303.
64. van Tilborg E, van Kammen CM, de Theije CGM, van Meer MPA, Dijkhuizen RM, Nijboer CH. A quantitative method for microstructural analysis of myelinated axons in the injured rodent brain. Sci Rep. 2017 Dec;7(1):16492.
65. Koenig SH. Cholesterol of myelin is the determinant of gray-white contrast in MRI of brain. Magn Reson Med. 1991 Aug;20(2):285–91.
66. Andrews DS, Lee JK, Solomon M, Rogers SJ, Amaral DG, Nordahl CW. A diffusion-weighted imaging tract-based spatial statistics study of autism spectrum disorder in preschool-aged children. J Neurodevelop Disord. 2019 Dec;11(1):32.
67. The IBIS Network, Wolff JJ, Swanson MR, Elison JT, Gerig G, Pruett JR, et al. Neural circuitry at age 6 months associated with later repetitive behavior and sensory responsiveness in autism. Molecular Autism. 2017 Dec;8(1):8.
68. Hong S-J, Hyung B, Paquola C, Bernhardt BC. The Superficial White Matter in Autism and Its Role in Connectivity Anomalies and Symptom Severity. Cerebral Cortex. 2019 Sep 13;29(10):4415–25.
69. Marques JP, Kober T, Krueger G, van der Zwaag W, Van de Moortele P-F, Gruetter R. MP2RAGE, a self bias-field corrected sequence for improved segmentation and T1-mapping at high field. NeuroImage. 2010 Jan;49(2):1271–81.
70. Hilbert T, Sumpf TJ, Weiland E, Frahm J, Thiran J-P, Meuli R, et al. Accelerated T_2 mapping combining parallel MRI and model-based reconstruction: GRAPPATINI: Accelerated T_2 Mapping. J Magn Reson Imaging. 2018 Aug;48(2):359–68.

Figures

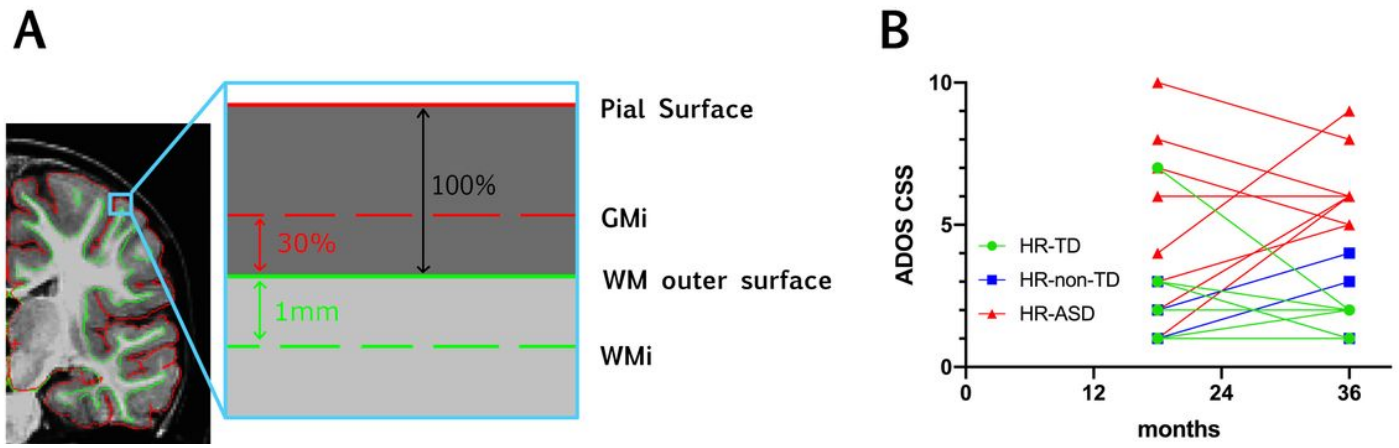

Figure 1

A. schematic representation of how GWC is computed at each vertex. GMi : grey matter intensity, WM: white matter, WMi: WM intensity. B. Graphic representation of individual ADOS CSS at 18 and 24 months of age in our sample (n=20 HR participants). Color code represents individual diagnosis outcome at age 3. HR-TD: high risk for ASD with typical development; HR-non-TD: high risk for ASD with atypical development; HR-TD: high risk for ASD with ASD.

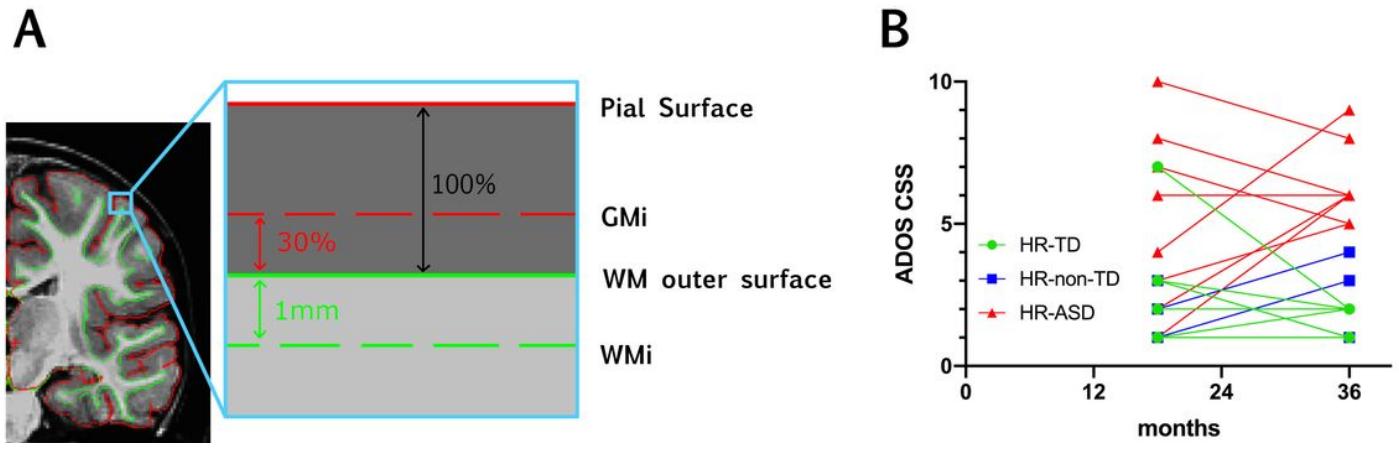

Figure 1

A. schematic representation of how GWC is computed at each vertex. GMi : grey matter intensity, WM: white matter, WMi: WM intensity. B. Graphic representation of individual ADOS CSS at 18 and 24 months of age in our sample (n=20 HR participants). Color code represents individual diagnosis outcome at age 3. HR-TD: high risk for ASD with typical development; HR-non-TD: high risk for ASD with atypical development; HR-TD: high risk for ASD with ASD.

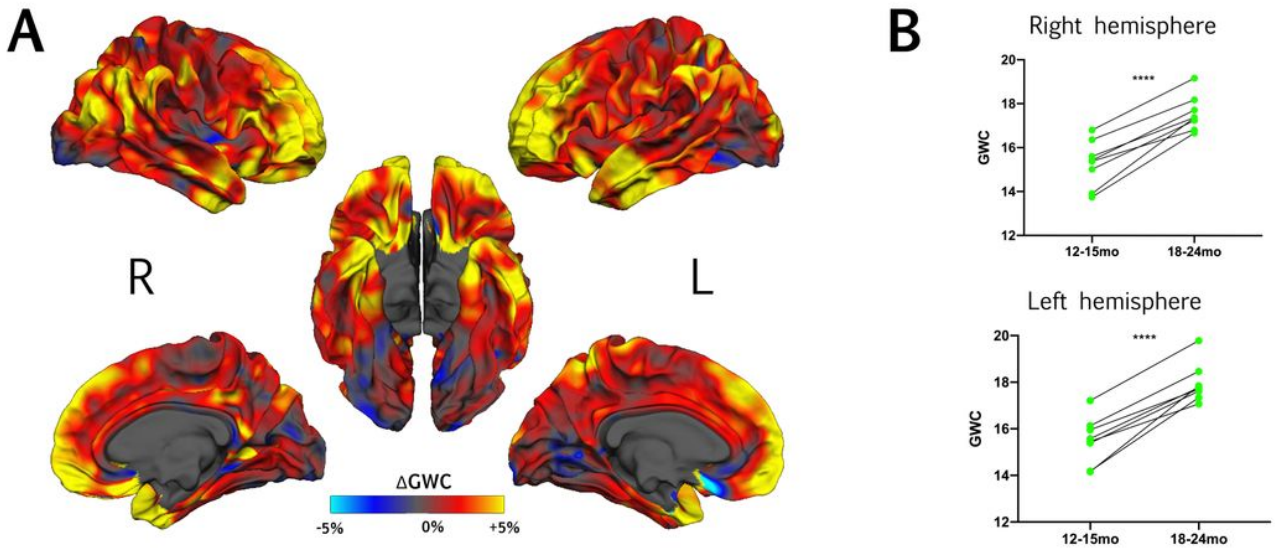

Figure 2

A. Effect of time on GWC within HR toddlers with typical development outcomes at 3 years (HR-TD) represented with vertex-wise ΔGWC values mapped on the common FreeSurfer template. B. For each hemisphere, individual trajectories of gray-white matter contrast (GWC) from 12-15 to 18-24 months within the HR-TD group. Individual GWC displayed are the average of all vertex-wise values extracted from clusters with a significant effect of time on GWC (one per hemisphere, see supplementary material S1). Right hemisphere: 12-15-mo GWC = 15.3% ± 1.1 ; 18-24 GWC = 17.6% ± 0.8. left hemisphere: 12-15mo GWC = 15.5% ± 1.0 ; 18-24-mo GWC = 17.9% ± 0.8. ****p<0.0001 (Student T-test).

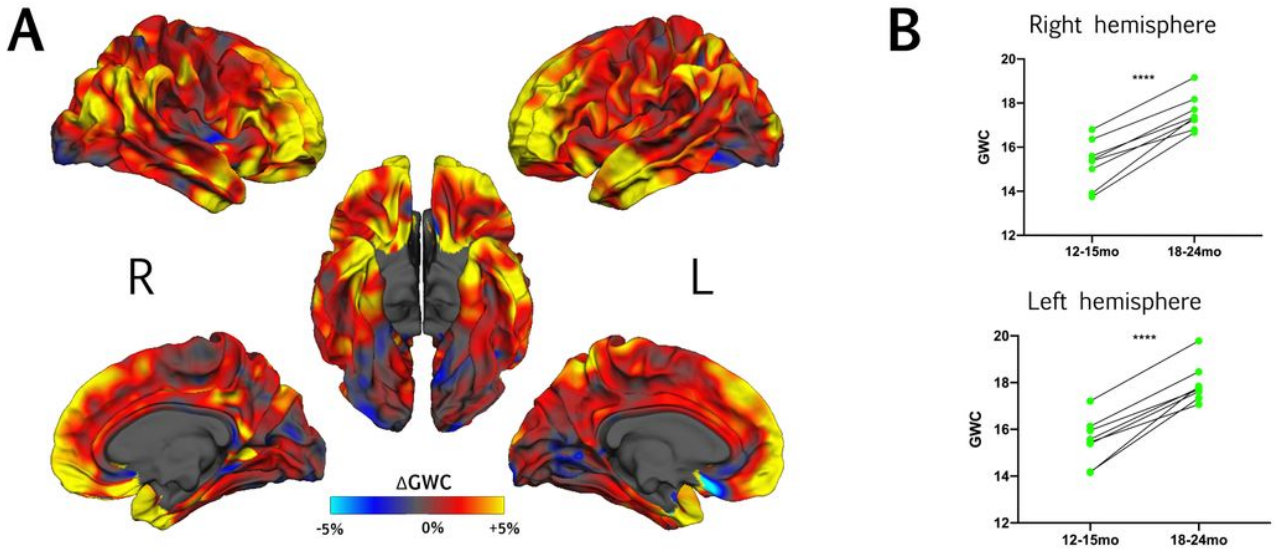

Figure 2

A. Effect of time on GWC within HR toddlers with typical development outcomes at 3 years (HR-TD) represented with vertex-wise ΔGWC values mapped on the common FreeSurfer template. B. For each hemisphere, individual trajectories of gray-white matter contrast (GWC) from 12-15 to 18-24 months within the HR-TD group. Individual GWC displayed are the average of all vertex-wise values extracted from clusters with a significant effect of time on GWC (one per hemisphere, see supplementary material S1). Right hemisphere: 12-15-mo GWC = 15.3% ± 1.1 ;

18-24 GWC = 17.6% ± 0.8. left hemisphere: 12-15mo GWC = 15.5% ± 1.0 ; 18-24-mo GWC = 17.9% ± 0.8. ****p<0.0001 (Student T-test).

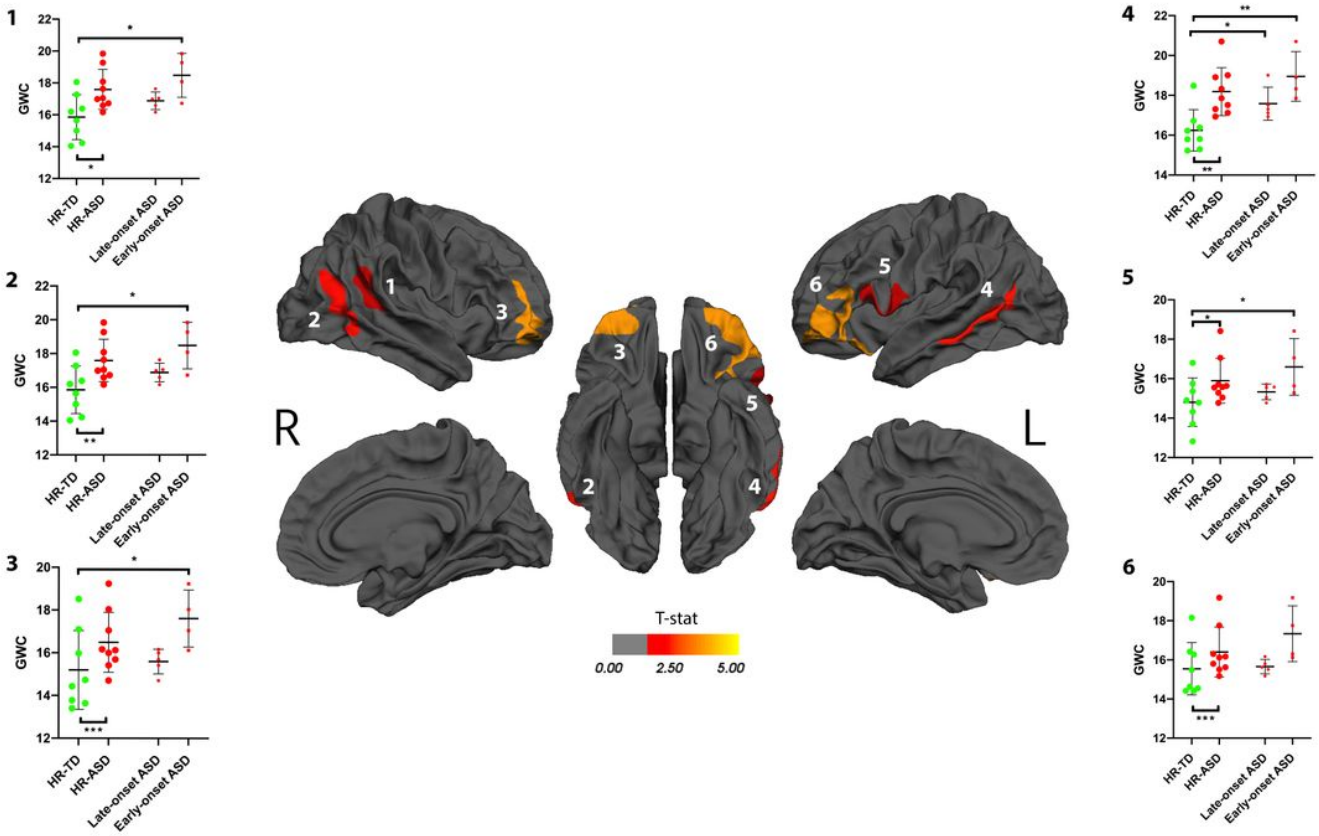

Figure 3

Clusters in which gray-white matter contrast (GWC) at age 12-24 months (computed as mean GWC between the two scan acquisitions) has a significant association with diagnostic outcome at age 3 (HR-TD or HR-ASD). Only clusters with CWP < 0.05 after regression for age are and correction for multiple comparisons are displayed. Within each hemisphere, clusters are numbered in order of decreasing effect size (Cohen's D, see table 2). Color code corresponds to p-value of the vertex with the greatest p-value within the cluster. P-values are represented as T-stat = -log(p-value). On the sides, individual mean GWC values for each significant cluster are displayed. Values of HR-ASD participants are further split into LOA and EOA subgroups on the right of each graph.). *p<0.05 **p<0.01 ***p<0.001.

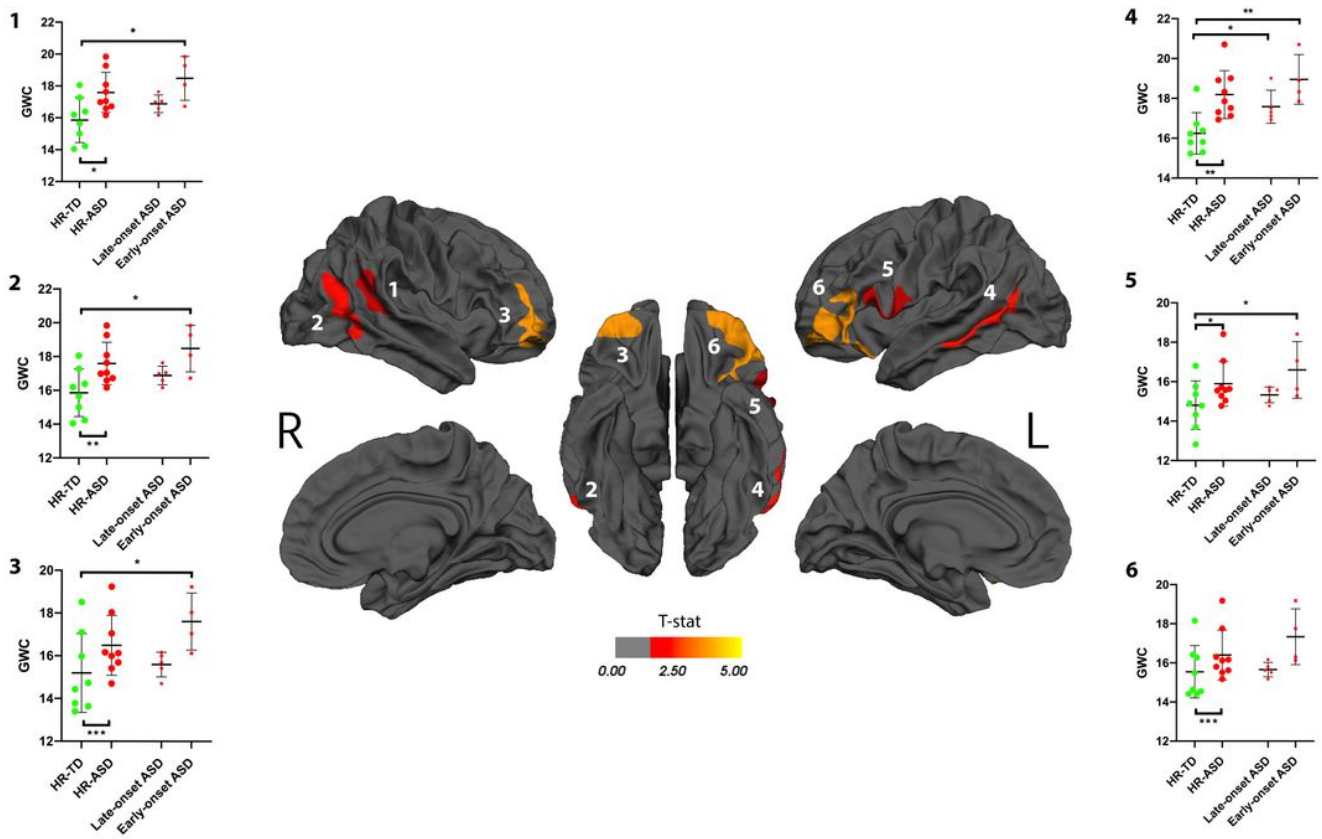

Figure 3

Clusters in which gray-white matter contrast (GWC) at age 12-24 months (computed as mean GWC between the two scan acquisitions) has a significant association with diagnostic outcome at age 3 (HR-TD or HR-ASD). Only clusters with CWP < 0.05 after regression for age are and correction for multiple comparisons are displayed. Within each hemisphere, clusters are numbered in order of decreasing effect size (Cohen's D, see table 2). Color code corresponds to p-value of the vertex with the greatest p-value within the cluster. P-values are represented as T-stat = -log(p-value). On the sides, individual mean GWC values for each significant cluster are displayed. Values of HR-ASD participants are further split into LOA and EOA subgroups on the right of each graph.). *p<0.05 **p<0.01 ***p<0.001.

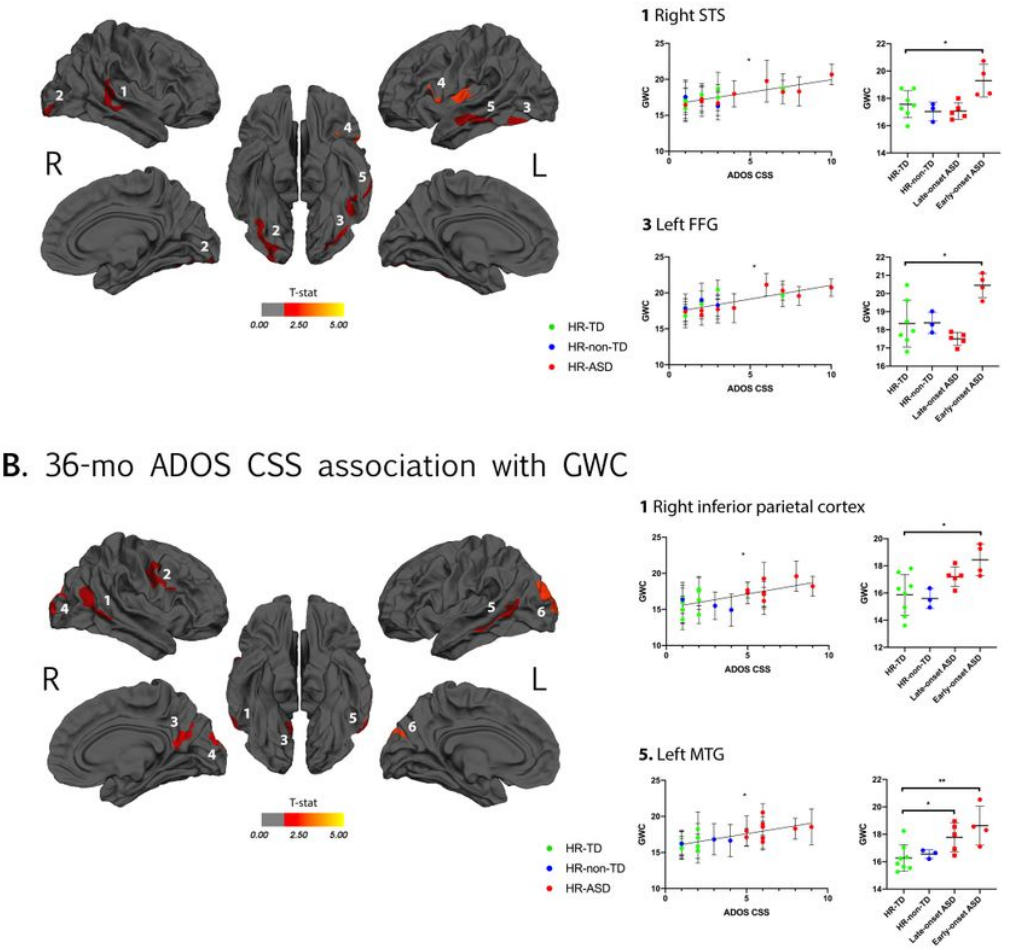

Figure 4

A. Clusters with a significant association between gray-white matter contrast (GWC) at age 12-24 months (computed as mean GWC between two scan acquisitions) and ADOS calibrated severity score (CSS) at 18 months of age. Only clusters with CWP < 0.05 after regression for age and correction for multiple comparisons are displayed. Color code correspond to P-value of the vertex with maximal p-value (Pvm) of each cluster and is represented as T-stat values (see table 2). Within each hemisphere, clusters are listed in order of decreasing effect size (Pearson's R, see table 2). On the right, individual mean GWC values are displayed in function of ADOS CSS for clusters with the greatest effect size. Same individual values are further plotted on the right in function of diagnostic outcome group (HR-TD, HR-non-TD) and HR-ASD subgroups (LOA and EOA). Results of

comparisons between LOA/EOA and HR-TD are displayed on the same graph. Similar graphs for all significant clusters are available in supplementary material (S2A). B. Association between GWC at age 12-24 months of age and symptom severity at 36 months of age. Detailed results for all clusters are displayed in supplementary material (S2B) C. Clusters of figures 4A and 4B displayed on a common template with color code corresponding to the age of clinical assessment (green for 18 and blue for 36 months of age). *p<0.05 **p<0.01. mGWC: mean GWC between the two scan acquisitions.

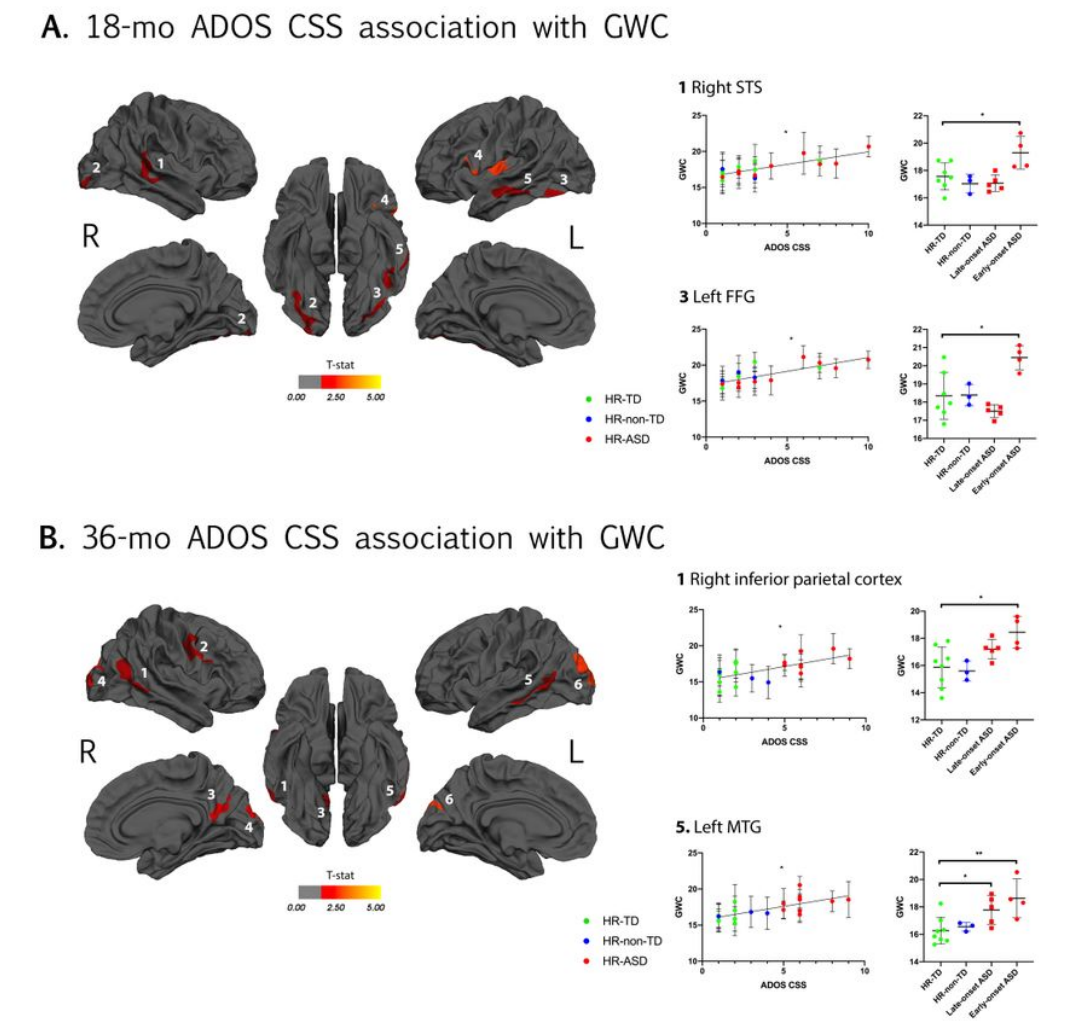

Figure 4

A. Clusters with a significant association between gray-white matter contrast (GWC) at age 12-24 months (computed as mean GWC between two scan acquisitions) and ADOS calibrated severity score (CSS) at 18

months of age. Only clusters with CWP < 0.05 after regression for age and correction for multiple comparisons are displayed. Color code correspond to P-value of the vertex with maximal p-value (Pvm) of each cluster and is represented as T-stat values (see table 2). Within each hemisphere, clusters are listed in order of decreasing effect size (Pearson's R, see table 2). On the right, individual mean GWC values are displayed in function of ADOS CSS for clusters with the greatest effect size. Same individual values are further plotted on the right in function of diagnostic outcome group (HR-TD, HR-non-TD) and HR-ASD subgroups (LOA and EOA). Results of comparisons between LOA/EOA and HR-TD are displayed on the same graph. Similar graphs for all significant clusters are available in supplementary material (S2A). B. Association between GWC at age 12-24 months of age and symptom severity at 36 months of age. Detailed results for all clusters are displayed in supplementary material (S2B) C. Clusters of figures 4A and 4B displayed on a common template with color code corresponding to the age of clinical assessment (green for 18 and blue for 36 months of age). *p<0.05 **p<0.01. mGWC: mean GWC between the two scan acquisitions.

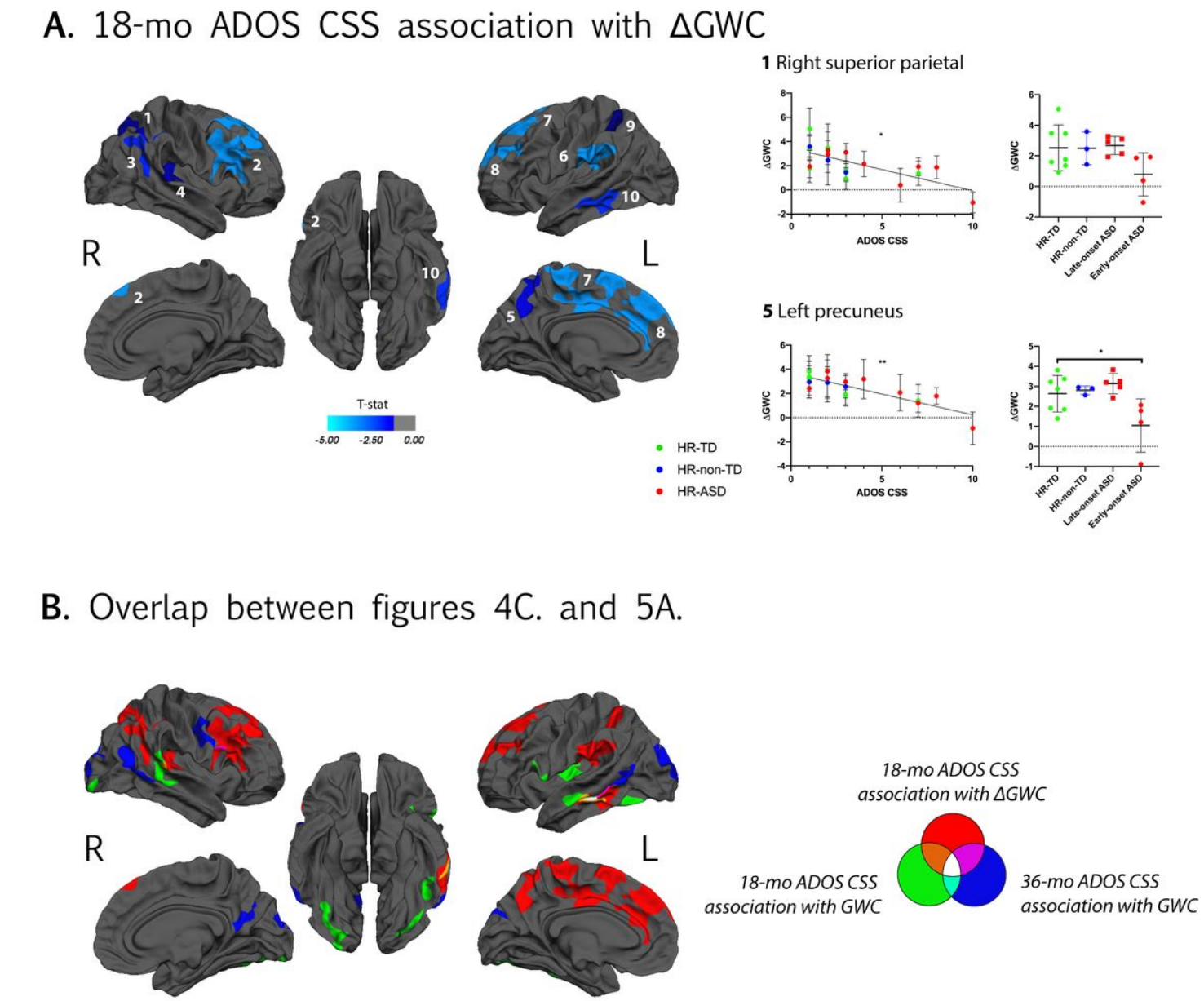

Figure 5

A. Association between GWC rate of change (ΔGWC) between 12 and 24 months of age and ADOS calibrated severity score (CSS) at 18 months of age. Only clusters with CWP < 0.05 after regression for age and correction for multiple comparisons are displayed. Color code correspond to P-value of the vertex with maximal P-value (Pvm) of each cluster (see table 2). In each hemisphere, clusters are listed in order of decreasing effect size (Pearson's R, see table 2). On the right, individual ΔGWC are displayed in function of ADOS CSS. Only values for clusters with the greatest effect sizes are shown. Same individual values are further plotted on the right in function of diagnostic outcome group (HR-TD, HR-non-TD and HR-ASD) and HR-ASD subgroups (LOA and EOA). Results of comparisons between LOA/EOA and HR-TD are displayed on the same graph. Similar graphs for all significant clusters are displayed in supplementary material (S3). B. Clusters displayed on Fig 5A and clusters with a significant association between GWC at age 12-24 months and ADOS CSS at 18 months and 36 months of age (Fig 4C) displayed on a common template. Color code reflects which longitudinal GWC value (either mean GWC or ΔGWC) and which ADOS CSS (either at 18 months or 36 months of age) were used in GLM. *p<0.05 **p<0.01.

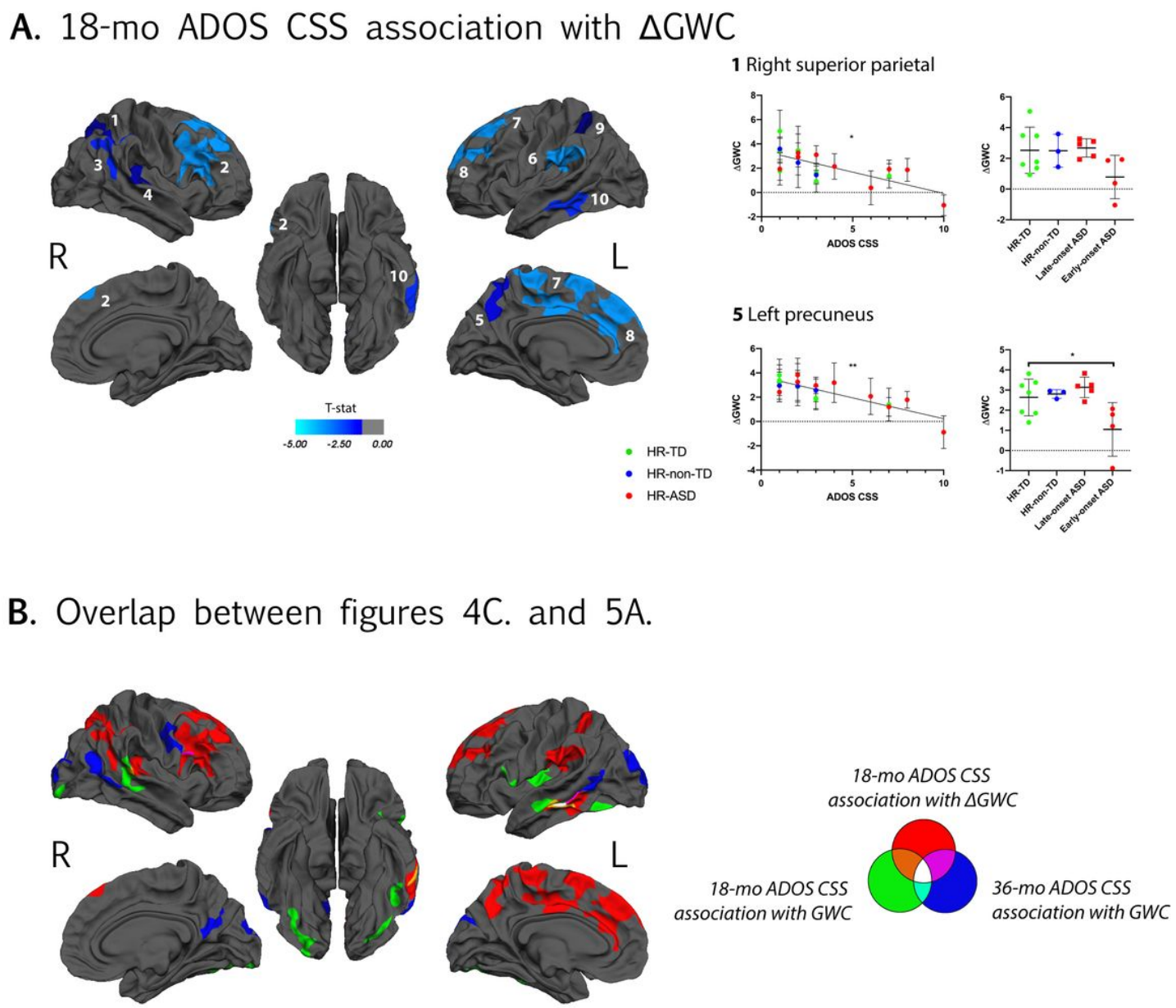

Figure 5

A. Association between GWC rate of change (ΔGWC) between 12 and 24 months of age and ADOS calibrated severity score (CSS) at 18 months of age. Only clusters with CWP < 0.05 after regression for age and correction for multiple comparisons are displayed. Color code correspond to P-value of the vertex with maximal P-value (Pvm) of each cluster (see table 2). In each hemisphere, clusters are listed in order of decreasing effect size (Pearson's R, see table 2). On the right, individual ΔGWC are displayed in function of ADOS CSS. Only values for clusters with the greatest effect sizes are shown. Same individual values are further plotted on the right in function of diagnostic outcome group (HR-TD, HR-non-TD and HR-ASD) and HR-ASD subgroups (LOA and EOA). Results of comparisons between LOA/EOA and HR-TD are displayed on the same graph. Similar graphs for all significant clusters are displayed in supplementary material (S3). B. Clusters displayed on Fig 5A and clusters with a significant association between GWC at age 12-24 months and ADOS CSS at 18 months and 36 months of age (Fig 4C) displayed on a common template. Color code reflects which longitudinal GWC value (either mean GWC or ΔGWC) and which ADOS CSS (either at 18 months or 36 months of age) were used in GLM. *p<0.05 **p<0.01.

Supplementary Files

This is a list of supplementary files associated with this preprint. Click to download.

- S1.jpg
- S1.jpg
- S2.jpg
- S2.jpg
- S3.jpg
- S3.jpg
- S4.jpg
- S4.jpg